Acta Crystallographica Section B
Structural Science
ISSN 0108-7681

On the structure of aragonite

E. N. Caspi,[a]* B. Pokroy,[b] P. L. Lee,[c] J. P. Quintana[d] and E. Zolotoyabko[b]

[a]Physics Department, Nuclear Research Centre–Negev, PO Box 9001, Beer-Sheva 84190, Israel, [b]Department of Materials Engineering, Technion Israel Institute of Technology, Haifa 32000, Israel, [c]X-ray Operation and Research, Advanced Photon Source, Argonne National Laboratory, 9700 South Cass Avenue, Argonne, IL 60439, USA, and [d]DND-CAT Synchrotron Research Center, Northwestern University, APS/ANL Sector 5, Building 432A, 9700 South Cass Avenue, Argonne, IL 60439-4857, USA

Correspondence e-mail: caspie@nrcn.org.il

Received 25 July 2004
Accepted 16 February 2005

High-resolution synchrotron powder diffraction measurements were carried out at the 32-ID beamline of the Advanced Photon Source of Argonne National Laboratory in order to clarify the structure of geological aragonite, a widely abundant polymorph of $CaCO_3$. The investigated crystals were practically free of impurity atoms, as measured by wavelength-dispersive X-ray spectroscopy in scanning electron microscopy. A superior quality of diffraction data was achieved by using the 11-channel 111 Si multi-analyzer of the diffracted beam. Applying the Rietveld refinement procedure to the high-resolution diffraction spectra, we were able to extract the aragonite lattice parameters with an accuracy of about 20 p.p.m. The data obtained unambiguously confirm that pure aragonite crystals have orthorhombic symmetry.

1. Introduction

The structure of aragonite, the orthorhombic polymorph of $CaCO_3$, continues to attract the attention of researchers 80 years after its first determination by W. L. Bragg in 1924 (Bragg, 1924). This is due to the widespread abundance of aragonite and its important role in geochemistry and especially in biomineralization (Lowenstam & Weiner, 1989). The latter field is studied intensively worldwide with the aim of understanding the secrets of the materials with superior characteristics often produced by living organisms. The key issue is the interaction between organic macromolecules, supplied by an organism, and a ceramic matrix, in this case $CaCO_3$. It is commonly believed that the organic molecules are responsible for the precise control of the morphology and orientation of the crystallites during the growth of biogenic crystals (see *e.g.* Berman *et al.*, 1988).

Organic macromolecules incorporated in the ceramic matrix result in local deformation fields, which can be a source of lattice distortions (Pokroy *et al.*, 2004). It is therefore extremely important to know the structure of aragonite of non-biogenic (for example, geological) origin as a reference for comparison with biogenic crystals. However, despite numerous studies (see Bevan *et al.*, 2002, and references therein) the subject is still controversial. Even the type of aragonite structure is being debated. Although careful measurements in the 1970s (Dal Negro & Ungaretti, 1971; De Villiers, 1971) confirmed the orthorhombic symmetry of aragonite, most recent single-crystal diffraction measurements (Bevan *et al.*, 2002) revealed a number of forbidden reflections, which should not occur within orthorhombic symmetry. As claimed by Bevan and co-workers, their results indicate the triclinic symmetry of the aragonite lattice. Note that the orthorhombic unit cell can be transformed into the triclinic

Table 1
Impurity concentrations in geological aragonite detected by WDS.

Element	Concentration (at. %)	Detection limit, C_{lim} (p.p.m.)
Sr	0.058 ± 0.002	23
Al	0.045 ± 0.006	15
Na	0.027 ± 0.006	44
Mg	0.013 ± 0.005	25

one by applying deformation, which is characterized by the non-zero non-diagonal components of the strain tensor (shear deformation). In principle, such a deformation can be introduced by impurity atoms or by other point defects (see *e.g.* Shilo *et al.*, 2001).

In order to shed additional light on the subject, we performed high-resolution synchrotron powder diffraction measurements with geological aragonite from Sefrou (Morocco), which was found to be almost free of impurity atoms. As compared with single-crystal diffraction, powder diffraction measurements do not show double diffraction peaks, which can be erroneously attributed to certain forbidden reflections due to the Renninger effect. Besides that, crushing single crystals to a fine powder allows us to remove the residual stresses that may arise in a single crystal due to the differences in temperature and other growth conditions at the surface and in the crystal interior. In order to significantly increase the angular resolution of powder diffraction, we used a diffraction instrument equipped with the advanced analyzing optics of the diffracted beam (see below). Applying Rietveld refinement to the diffraction spectrum of superior quality, we were able to extract the aragonite lattice parameters with an accuracy of *ca* 20 p.p.m. Our results indisputably confirm the orthorhombic symmetry of the aragonite crystals, at least those that can be considered as being practically free of impurities.[1]

2. Experimental

2.1. Chemical analysis

Since structural distortions can be induced by impurity atoms, careful measurement of their concentrations is of great importance. For chemical analysis, we used energy-dispersive spectroscopy (EDS) and wavelength-dispersive X-ray spectrometry (WDS) in the scanning electron microscope (Philips XL30 SEM) equipped with the EDS/WDS Link (Isis, Oxford Instruments). Before conducting the measurements, the crystal pieces were carefully washed and sonicated in 3% NaOH, followed by extensive washing in double-distilled water (DDW). After that, the samples were preliminarily monitored by EDS in order to find the impurities of the highest significance, whose concentrations were then precisely determined by WDS. Depending on the particular X-ray line, the WDS analysis was performed in 10–14 local regions of the sample, specifically on well developed 001-aragonite planes clearly visible in SEM. The final concentrations were determined by averaging the sets of measured data. The results obtained are summarized in Table 1, where the atomic concentrations of the detected impurities (in descending order) as well as the detection limits, C_{lim} (in p.p.m.), for a confidence probability of $P = 0.95$, are given. As follows from Table 1, the aragonite crystals are virtually free of impurity atoms; the highest concentration (of Sr) being less than 0.06 at. %.

2.2. High-resolution X-ray powder diffraction

For diffraction measurements, the aragonite crystals were cleaned by sonication in methanol and DDW and then air-dried. The aragonite powders were produced by crushing with a mortar and pestle followed by sieving through a 25 μm sieve. Powders were loaded into capillaries. To avoid intensity spikes from the individual grains subjected to quasi-parallel beam irradiation, the samples were rotated during measurements at a rate of 2 r.p.s.

Synchrotron diffraction measurements were performed at the 32-ID beamline of the Advanced Photon Source at the Argonne National Laboratory equipped with a two-circle Huber diffractometer combined with multi-channel analyzing optics. X-rays from the synchrotron storage ring were monochromated by the water-cooled double-crystal diamond monochromator. The optics of the diffracted beam consisted of eleven 111 Si crystal analyzers which could be separately adjusted. With 11 crystals in parallel, the efficiency of the detecting system is increased drastically, while an angular range to be scanned by the analyzing array is drastically reduced. The use of the advanced analyzing optics resulted in diffraction spectra of superior quality and above all in extremely narrow diffraction peaks with an instrumental contribution to the peak widths not exceeding 0.004° (see *e.g.* Fitch, 2004).

The calibration of the instrument and refinement of the wavelength [λ = 0.49581 (1) Å] were performed with the silicon standard sample from *NIST*.

3. Results and discussion

A selected part of the high-resolution diffraction spectrum taken from geological aragonite and containing the most significant diffraction peaks is shown in Fig. 1. The whole spectrum was collected within an angular interval of $5 < 2\theta < 54°$. The vast majority of observed reflections were attributed to the main aragonite phase of orthorhombic symmetry. Owing to the high statistics and superior angular resolution, we were able to detect the 102 aragonite diffraction peak at $2\theta = 11.449°$ (see insert in Fig. 1). It is allowed for the orthorhombic system but is not mentioned in the updated JCPDS file 41-1475, most probably because of very close location to the 200 diffraction peak. Additional tiny non-aragonitic reflections were attributed to the calcite (rhombohedral polymorph of $CaCO_3$) phase and α-quartz contamination phase, comprising 3.52 (2) and 0.23 (1) wt %,

[1] Supplementary data for this paper are available from the IUCr electronic archives (Reference: LC5015). Services for accessing these data are described at the back of the journal.

respectively, as determined by Rietveld analysis (see below). Neither extra diffraction peaks nor a broadening or splitting of selected aragonite reflections, which could indicate symmetry lower than orthorhombic for aragonite phase, was observed.

A Rietveld refinement was performed within the *GSAS* program (Larson & Von Dreele, 2004), using the EXPGUI interface (Toby, 2001) with the Thompson–Cox–Hastings pseudo-Voigt peak-shape functions (Thompson *et al.*, 1987), the Finger–Cox–Jephcoat asymmetry correction (Finger *et al.*, 1994) and the Stephens microstrain profile broadening function (Stephens, 1999). The refined model utilized 37 structural parameters and 41 instrumental and background parameters. Using the Rietveld method, the experimental diffraction spectrum was successfully described within the orthorhombic *Pmcn* (No. 62) structural model with the following atomic positions: Ca, C and O1 at 4(*c*) ($\frac{1}{4}$, *y*, *z*), and O2 at 8(*d*) (*x*, *y*, *z*). The high quality of experimental data (including both statistics and angular resolution) also allowed us to refine the squares of the anisotropic thermal displacements, U^{ij}, of the aragonite atoms. The calcite and α-quartz phases were introduced into the refined model, using previously published structural data (Wartchow, 1989; Ogata *et al.*, 1987). Based on the peak widths, one can say that the calcite phase exists in the form of nanometre-size crystals, which most probably represent calcite precipitates formed at a certain stage of the geological process in competition with aragonite formation. A small amount of α-quartz in the sample represents natural contamination of geological aragonite which is visible in elemental maps taken by EDS in SEM.

The unit-cell parameters, atomic positions and anisotropic displacement parameters of the aragonite phase are summarized in Table 2. The numbers in parentheses represent one standard deviation in the least significant digit, as deduced from Rietveld analysis. The achieved agreement factors, R_{wp} = 0.0547 and R_{exp} = 0.0209, indicate excellent agreement between the refined model and the measured diffraction spectrum.

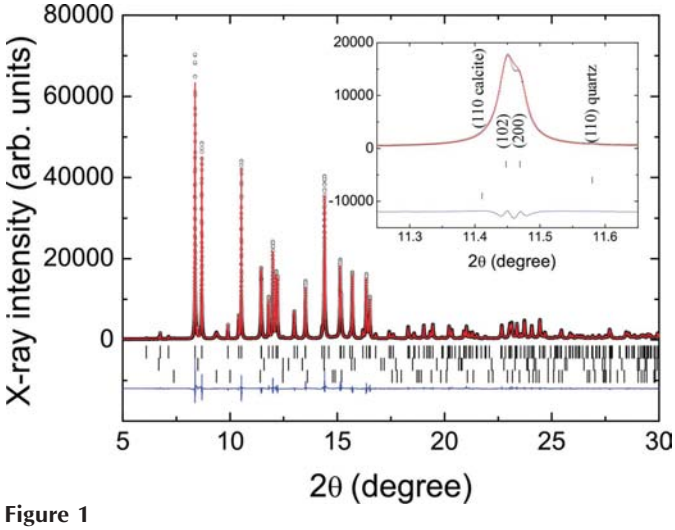

Figure 1
Part of the measured high-resolution X-ray diffraction spectrum of powdered geological aragonite (open circles) superimposed on the best-fit calculated Rietveld refinement profile (solid line) and their difference (solid line at the bottom). Upper, middle and lower rows of tick marks represent Bragg positions of aragonite, α-quartz and calcite reflections, respectively. The insert shows two closely related diffraction peaks, 200 (on the right) and 102 (on the left), the latter missing in the JCPDS file 41–1475.

Table 2
Refined room-temperature structural parameters of geological $CaCO_3$.

The U^{ij} values are the squares of the anisotropic atomic displacements in units of Å^2. R_p, R_{wp}, R_{exp} and R_{F^2} are the profile, weighted profile, expected and observed structure-factor agreement factors, respectively, as deduced from the Rietveld analysis.

a (Å)	4.96183 (1)
b (Å)	7.96914 (2)
c (Å)	5.74285 (2)
V (Å^3)	227.081 (1)
Ca (4*c*)	
y	0.41502 (2)
z	0.75985 (4)
U^{11} (Å^2)	0.00450 (9)
U^{22} (Å^2)	0.00677 (9)
U^{33} (Å^2)	0.0117 (1)
U^{23} (Å^2)	−0.0020 (1)
C (4*c*)	
y	0.7619 (1)
z	−0.0823 (1)
U^{11} (Å^2)	0.0197 (6)
U^{22} (Å^2)	0.0210 (6)
U^{33} (Å^2)	0.0049 (5)
U^{23} (Å^2)	−0.005 (5)
O1 (4*c*)	
y	0.92238 (8)
z	−0.09453 (8)
U^{11} (Å^2)	0.0127 (4)
U^{22} (Å^2)	0.0033 (3)
U^{33} (Å^2)	0.0188 (4)
U^{23} (Å^2)	0.0037 (3)
O2 (8*d*)	
x	0.47499 (7)
y	0.68013 (5)
z	−0.08725 (7)
U^{11} (Å^2)	0.0004 (2)
U^{22} (Å^2)	0.0107 (2)
U^{33} (Å^2)	0.0200 (3)
U^{12} (Å^2)	0.0067 (2)
U^{13} (Å^2)	0.0003 (2)
U^{23} (Å^2)	0.0016 (2)
R_p	0.0412
R_{wp}	0.0547
R_{exp}	0.0209
R_{F^2}	0.0284
χ^2	6.85

The Rietveld refinement of lattice parameters yielded *a* = 4.96183, *b* = 7.96914, *c* = 5.74285 Å, which deviated from the values published in JCPDS file 41-1475 (*a* = 4.9623, *b* = 7.968, *c* = 5.7439 Å) by $\Delta a/a = -9.5 \times 10^{-5}$, $\Delta b/b = 1.4 \times 10^{-4}$ and $\Delta c/c = -1.8 \times 10^{-4}$. We consider the refined lattice parameters as more accurate than those published in the JCPDS database. Note that because of the use of analyzing optics in our measurements, the accuracy in the determination of lattice parameters is extremely high for the powder diffraction technique. Formally, based on standard deviations in Table 2, the precision of *ca* 2–4 p.p.m. could be deduced. However, taking into account that the absolute value of the X-ray

wavelength is defined within the standard deviation of 20 p.p.m. (see §2.2), the latter quantity better represents the precision of our measurements.

In addition, an attempt was made to fit the previously published triclinic model (Bevan *et al.*, 2002) to our experimental spectrum, which resulted in numerous calculated reflections with no experimental intensity. Moreover, in the framework of the triclinic model the refinement of the unit cell angles failed to converge, undoubtedly indicating the orthorhombic symmetry of aragonite. Therefore, in contrast to the work of Bevan *et al.* (2002), no reduction in symmetry was observed. We think that that discrepancy is a result of the high concentration of impurity atoms in the crystal used by Bevan *et al.* (2002). Among the 11 elements detected in that crystal, two elements, *viz.* Sr (n_{Sr} = 0.82 at. %) and Fe (n_{Fe} = 0.13 at. %), were found in much higher concentrations than in our sample (see Table 1).

Concerning Sr ions, it is known that they can substitute Ca ions without a change in structure to form strontium carbonate, $SrCO_3$. The latter shows lattice parameters which have increased on average by a factor of η = 4.5%, relative to $CaCO_3$ (Lippmann, 1973). Hence, we expect a lattice distortion, $\varepsilon_{Sr} = \eta \times n_{Sr} \simeq 4 \times 10^{-4}$, to be introduced by the Ca $\rightarrow$ Sr replacement.

Less is known about the specific positions of the Fe impurities within the aragonite unit cell. Nevertheless, a significant effect of Fe ions on lattice distortion in $CaCO_3$ is expected because of the great difference in ionic radii, $\Delta r/r \simeq$ 40–50%, between Fe and Ca ions (Shannon, 1976). A rough estimation of the induced lattice distortion yields: $\varepsilon_{Fe} = (\Delta r/r) \times n_{Fe} = 6 \times 10^{-4}$.

The (averaged) strain values obtained are three-to-four times lower than the critical strain of *ca* $\varepsilon = (S/E) \simeq 16 \times 10^{-4}$ [where $S \simeq 100$ MPa is the flexural strength and E = 60 GPa is the Young modulus (Kuhn-Spearing *et al.*, 1996)], which leads to the fracture of aragonite. However, lattice deformations will be much higher locally and perhaps high enough to trigger the orthorhombic-to-triclinic structural transformation in aragonite.

4. Summary

Our high-resolution powder diffraction measurements on the synchrotron beamline indisputably showed the orthorhombic symmetry of the aragonite lattice. The structural parameters obtained are similar to those given in various databases (JCPDS, Mineral Database *etc.*), albeit determined with much higher precision. In our opinion, the discrepancies in the determination of the aragonite symmetry are caused by the deformation fields induced by impurity atoms. The question about the possible role of impurities in the stabilization of triclinic aragonite was also raised in the Summary section of the paper by Bevan *et al.* (2002). Our measurements strengthen the point that pure enough aragonite (*e.g.* the one with impurity concentrations lower than 0.06 at. %, which we used) has orthorhombic symmetry. This is in agreement with early works (Dal Negro & Ungaretti, 1971; De Villiers, 1971), in which high-purity aragonite crystals were used for the diffraction measurements.

Use of the Advanced Photon Source was supported by the US Department of Energy, Basic Energy Sciences, Office of Science, under Contract No. W-31-109-Eng-38. The analyzing optics of the diffraction beam at the 32-ID beamline of APS was designed and built by K. D'Amico. This work was partially supported by the Israel Science Foundation founded by the Israel Academy of Science and Humanities. We thank Dr A. Berner (Technion) for his help with the WDS measurements. One of us (E.N.C.) would like to thank M. Y. Avdeev for helpful discussions.

References

Berman, A., Addadi, L. & Weiner, S. (1988). *Nature*, **331**, 546–548.
Bevan, D. J. M., Rossmanith, E., Mylrea, D. K., Ness, S. E., Taylor, M. R. & Cuff, C. (2002). *Acta Cryst.* B**58**, 448–456.
Bragg, W. L. (1924). *Proc. R. Soc. A (London)*, **105**, 16–39.
Dal Negro, A. & Ungaretti, L. (1971). *Am. Mineral.* **56**, 767–772.
De Villiers, J. P. R. (1971). *Am. Mineral.* **56**, 758–767.
Finger, L. W., Cox, D. E. & Jephcoat, A. P. (1994). *J. Appl. Cryst.* **27**, 892–900.
Fitch, A. N. (2004). *J. Res. Natl. Inst. Stand. Technol.* **109**, 133–142.
Kuhn-Spearing, L. T., Kessler, H., Chateau, E., Ballarini, R., Heuer, A. H. & Spearing, S. M. (1996). *J. Mater. Sci.* **31**, 6583–6594.
Larson, C. & Von Dreele R. B. (2004). *GSAS*. Report No. LAUR 86-748. Los Alamos National Laboratory, New Mexico, USA.
Lippmann, F. (1973). *Sedimentary Carbonate Minerals*, ch. B. Berlin: Springer.
Lowenstam, H. A. & Weiner, S. (1989). *On Biomineralization.* Oxford University Press.
Ogata, K., Takeuchi, Y. & Kudoh, Y. (1987). *Z. Kristallogr.* **179**, 403–413.
Pokroy, B., Quintana, J. P., Caspi, E. N., Berner, A. & Zolotoyabko, E. (2004). *Nature Mater.* **3**, 900–902.
Shannon, R. D. (1976). *Acta Cryst.* A**32**, 751–767.
Shilo, D., Lakin, E. & Zolotoyabko, E. (2001). *Phys. Rev. B*, **63**, 205420.
Stephens, P. W. (1999). *J. Appl. Cryst.* **32**, 281–289.
Thompson, P., Cox, D. E. & Hastings, J. B. (1987). *J. Appl. Cryst.* **20**, 79–83.
Toby, B. (2001). *J. Appl. Cryst.* **34**, 210–221.
Wartchow, R. (1989). *Z. Kristallogr.* **186**, 300–302.